Expanding the Modeling of Type Ia Supernovae

Abigail Bishop

ABSTRACT

Type Ia Supernovae are some of the most important astronomical events in the universe as they serve as standard candles that observational astronomers can use to make distance calculations. There are three main models of Type Ia supernovae, which include white dwarf mergers, sub-Chandrasekhar double detonations, and Chandrasekhar mass single detonations (Kromer et al. 2010; Fink et al. 2007). A paper by Ken Shen and Lars Bildsten reveals that the simulations which make these supernovae so valuable are not fully developed and may be leading to inaccuracies in measurements (Shen & Bildsten 2009). This report details the process by which nuclear astrophysics codes like Pynucastro, Microphysics, and Castro are used to test the claims of Shen & Bildsten by simulating Type Ia Supernovae using the sub-Chandrasekhar double detonation model. Currently, it is clear that the initial detonation is propagating through the helium layer of a sub-Chandrasekhar mass WD. As the simulation continues to progress we hope to see the second detonation then to move on to higher level simulations.

1. INTRODUCTION

Supernovae (SNe), the explosive deaths of stars, are some of the most spectacular events in the universe. A SNe typically occurs due to a thermonuclear explosion or a gravitational collapse. A special kind of thermonuclear supernovae, the Type Ia Supernovae, is especially notable for its use as an astronomical measure of distance. Type Ia supernovae occur when two stars are in orbit around each other where at least one star has already died once and has become a white dwarf (WD), usually with a mass around that of our sun ($M_\odot$). Material in the outer shells of the WD's partner can be stolen by the WD through its gravitational field. In the long standing theoretical model, once the WD has taken enough material to reach a mass of 1.4 times $M_\odot$, it explodes. This $1.4M_\odot$ is called the Chandrasekhar mass. The explosion releases light of many colors and other wavelengths. The graph plotting how bright each wavelength of light is in the explosion is the spectrum. Since these stars usually have the same mass and elemental composition when they explode, the explosions have the same brightness and uniquely Type Ia SNe spectrum characterized by a lack of Hydrogen and an abundance of Silicon (Phillips 1993).

An observational astronomer can observe an event resembling a Type Ia SNe and use its spectrum to confirm it is a Type Ia Supernovae. The astronomer can then take the brightness of the explosion and use it to calculate how far away the supernovae is. By using Type Ia SNe in other galaxies to measure how far away they are along with other measurements, observational cosmologists have been able to measure the rate at which our universe is expanding and note that the expansion rate is accelerating (Riess et al. 1998; Perlmutter et al. 1999). Without accurate models of Type Ia SNe, these calculations would not be possible.

The dilemma is that not all Type Ia Supernovae wait until their mass reaches the Chandrasekhar mass of $1.4M_\odot$ before they explode. Some explode at lower masses, in the sub-Chandra range where their mass is less than $1.4M_\odot$, through a mechanism called double-detonation (Kromer et al. 2010; Fink et al. 2007). Out of an increase in temperature, reactions in the Helium shell of a WD propel a shock wave through the WD's shell that hits the core of the WD causing a second detonation in the core. This difference in the explosion mechanism means the overall brightness and the spectrum of the explosion is slightly different from the Chandrasekhar mass Type Ia Supernovae. If an observational astronomer uses a sub-Chandra Type Ia supernovae to measure distance, they will calculate a larger distance if they assume it is a Chandrasekhar mass star. This means, as computational nuclear astrophysicists, we need to model sub-Chandra Type Ia SNe to help the observational astronomers make accurate calculations of astronomical distance. This has been done before, however, the paper Shen & Bildsten (2009) has pointed out that previous simulations have not included as many possible nuclear reactions as it should have to make the calculations accurate. In this thesis I discuss the methods by which we use a computer code to simulate Type Ia SNe with the nuclei and reactions suggested by Shen and Bildsten.

2. CODES

We use several codes developed by our group, all of which are available on GitHub. GitHub is a website used to mediate code sharing and code collaboration. Most of the codes discussed in this report available for viewing, editing, and using (also known as open-sourced software). This helps to promote reproducibility and encourages community contributions to the projects.

2.1. *Pynucastro*

Pynucastro is an open-sourced coding package developed by Dr. Michael Zingale and Dr. Donald Willcox to create networks of nuclear reactions that can be used in their simulations (Willcox & Zingale 2018). It does so by collecting information on the rate at which nuclear reactions occur at different temperatures from a database called the JINA Reaclib Database (Cyburt et al. 2010). Using the Pynucastro Python library, a script can be written that will incorporate specifically chosen JINA reaction rates into a model and rates that can be used in Microphysics and Castro simulations.

2.2. *Microphysics*

Microphysics is an open-sourced software, available on the StarKiller GitHub repository, with routines designed to incorporate aforementioned networks of reaction rates into astrophysical simulations (the StarKiller Microphysics Development Team et al. 2019). This is done through the solving of differential equations called the Equations of State then mapping the results into plots of star qualities like temperature, energy generation rate, and density. It is equipped with unit tests designed to run stellar simulations in a short amount of time to troubleshoot problems on a small scale before promoting the simulations to a larger scale operation. Microphysics comes with some preexisting networks but can also use new networks generated by Pynucastro.

2.3. *Castro*

Castro is an open sourced software, available under the AMReX-Astro repository on GitHub, and is designed to run full scale simulations of astrophysical events in one dimension, two dimensions, and three dimensions (Almgren et al. 2010). Castro is initialized with a model that includes a stellar

object and information about its density, temperature, and pressure. This code solves Equations of State; conservation of total mass, momentum, and energy and other hydrodynamics equations; and Poisson's equation for self gravity using a Strang Splitting technique (Strang 1968) to calculate the evolution of the initial model over time. All of these equations need to be solved for individual points on a line (for 1-Dimensional simulations), in a grid (2-D), or in a box (3-D) which is very time and computationally expensive. Adaptive Mesh Refinement (AMR) is used to assist with this as it will request that fewer equations be solved in regions of the simulation where there is less activity, but will also request that more equations be solved in very exciting regions leading to a more resolved and accurate picture. To further help with the computationally expensive nature of this process, Castro has been designed to run on supercomputers that can drastically cut the run time of these simulations. To date, Castro has been used to conduct many exciting simulations like Type Ia SNe (Zingale et al. 2013; Jacobs et al. 2016), core collapse SNe (Burrows et al. 2012; Dolence et al. 2013), and WD mergers (Katz et al. 2016).

3. MOTIVATION

As previously mentioned, Type Ia SNe are critical to measuring large astronomical distances. Observational astronomers rely heavily on accurate estimations for what they observe to make scientific claims to their data. In the paper Shen & Bildsten (2009), it is theorized that the three elements used to simulate Type Ia supernovae were not enough to accurately simulate the spectra and light curve of a Type Ia supernovae. Additionally, not all Type Ia SNe occur when the WD becomes a total of 1.4 $M_\odot$. In the double detonation model, Type Ia supernovae can occur in the sub-Chandrasekhar regime because a hot spot in the Helium layer of a WD causes a thermonuclear reaction runaway sending a shockwave through the Helium layer. This shock wave hits the Carbon-Oxygen core of the WD and initiates the Type Ia. Being sub-Chandrasekhar means that these SNe could have different observational signatures that Chandrasekhar mass Type Ia SNe. It is critical that accurate models of Type Ia SNe are obtained in order for observational astronomers to learn about the universe accurately.

The goal for this research is to first create a nuclear reaction network following Shen and Bildsten's guidelines, test the network in Microphysics to see if there is a substantial change, then to run a model without the elements and reactions suggested by Shen & Bildsten to be compared with a model that does consider their recommendations. If the change in results is drastic, then we will have sufficient motivation to conduct more detailed calculations to understand these consequences.

4. SIMULATIONS AND RESULTS

4.1. *Pynucastro*

`Aprox13` is a nuclear reaction network composed of 13 isotopes (Timmes 2019). It begins with Helium (^{4}He, also known as an α particle) adds two ^{4}He to get a Carbon (^{12}C) and one photon (γ) then continues to add α particles until Iron (^{56}Fe) and a lot more γ's are obtained. Since each isotope is connected by an α particle, this is called an α chain and earns the name 13 from the 13 isotopes on the α chain that it possesses. All elements that are ^{24}Mg and heavier are also connected through a process where an α particle hits an isotope and creates a new particle but kicks out a proton, then a different proton hits the new nucleus and one of those α chain isotopes are created along with a γ. In total the `aprox13` network contains 13 isotopes and has proven to be a good model

of stellar evolution, but Shen & Bildsten (2009) suggests adding additional rates to the beginning of this double-detonation model for Type IaSNe.

This study began through the use of Pynucastro to create the `subch` network, standing for sub-Chandrasekhar. The network is composed of 8 reactions and 11 isotopes, with Chemical Equations 3, 4, 5, 6, and 8 being the ones suggested by Shen & Bildsten (2009) and the remaining three being a part of the α chain processes. The big change made through the generation of this network is the addition of ^{14}C and ^{14}N which will be the key players in expediting the explosion in this model.

$$3\,^{4}\text{He} \longrightarrow {}^{12}\text{C} + 2\,\gamma \tag{1}$$

$$^{12}\text{C} + {}^{4}\text{He} \longrightarrow {}^{16}\text{O} + \gamma \tag{2}$$

$$^{14}\text{N} + {}^{4}\text{He} \longrightarrow {}^{18}\text{F} + \gamma \tag{3}$$

$$^{18}\text{F} + {}^{4}\text{He} \longrightarrow {}^{21}\text{Ne} + \text{p}^{+} \tag{4}$$

$$^{12}\text{C} + \text{p}^{+} \longrightarrow {}^{13}\text{N} + \gamma \tag{5}$$

$$^{13}\text{N} + {}^{4}\text{He} \longrightarrow {}^{16}\text{O} + \text{p} \tag{6}$$

$$^{16}\text{O} + {}^{4}\text{He} \longrightarrow {}^{20}\text{Ne} + \gamma \tag{7}$$

$$^{14}\text{C} + {}^{4}\text{He} \longrightarrow {}^{18}\text{O} + \gamma \tag{8}$$

4.2. Microphysics

This new network is now used in Microphysics. There is a unit test in Microphysics referred to as `burn_cell` which simulates the chemical evolution in one small zone of a star. This test is first used to determine what tolerance will optimize results and reduce computation time in this simulation. Using these results, the `burn_cell` test will be used to simulate the chemical evolution of this zone as nuclear reactions take place to use and generate different elemental isotopes.

4.2.1. Testing Simulation Equation Tolerances

Tolerances are parameters used to gauge how accurately the ordinary differential equation solvers in the simulation are doing their job. These equations are all coupled and integrated numerically, so a good accuracy is critical. A smaller tolerance typically leads to a more precise answer but takes more computer time. For this reason, a tolerance of 10^{-12} was treated as an exact answer since it is very small but still significantly more than round off error (10^{-16}). The tolerances of 10^{-3}, 10^{-6}, and 10^{-9} were tested with respect to the test with a tolerance of 10^{-12}.

To test these tolerances, ^{4}He was initialized in one zone as modeled by the `burn_cell` unit test. The zone is heated so that the ^{4}He begins to burn into ^{12}C and ^{16}O. Simulations are run with a tolerance of 10^{-3}, 10^{-6}, 10^{-9}, and 10^{-12} in a zone that is initialized to a temperature of $T = 3 \times 10^{8} K$ and a density of $\rho = 1 \times 10^{6} \frac{g}{cm^{3}}$. The relative error in each element's mass fraction, X, is calculated between the 3 simulations with looser tolerances and the 10^{-12} simulation, as defined by

$$\sigma_X = \frac{|X_{10^{-12}} - X_{\text{former}}|}{X_{10^{-12}}} \;, \tag{9}$$

for each point in time during the simulation. This relative error in mass fraction is plotted as a function of time for each of the three testing simulations and can be seen in Figure 1.
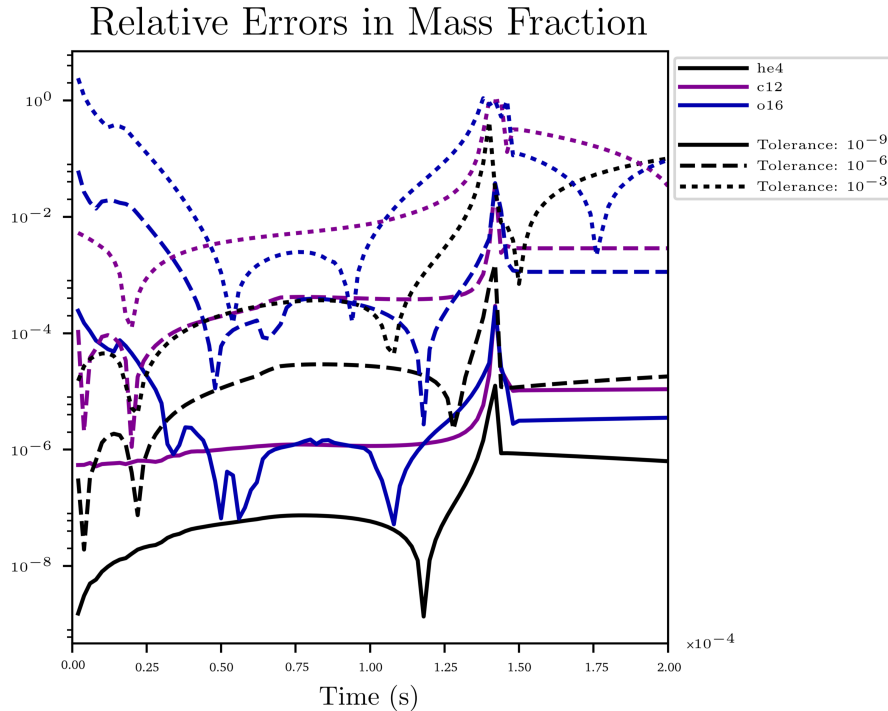
Figure 1. Relative error over time of the ^{4}H (in black), ^{12}C (in purple), and ^{16}O (in blue) mass fractions run in simulations with a tolerance of 10^{-9} (solid line), 10^{-6} (dashed line), and 10^{-3} (dotted line) calculated with respect to the true values calculated by a simulation with a tolerance of 10^{-12}. The lower the value, the closer the result is to the true value.

From Figure 1, one can see that the solid lines, corresponding with the simulation using a tolerance of 10^{-9}, are consistently the lowest. The relative error of the simulation with a tolerance of 10^{-9} is consistently below 10^{-3} and drops as low as 10^{-8} at times without taking much longer to run than the simulations with tolerances of 10^{-6} and 10^{-3}. Therefore, it is concluded that a tolerance of 10^{-9} is acceptable for the codes going forwards.

4.2.2. *Using Mass Fraction Evolution to Justify Motivation*

The next step with the `burn_cell` tests is to test if the `subch` network is producing results worth investigating. The main ingredients to the simulation that Shen & Bildsten encouraged were ^{14}C and ^{14}N (Shen & Bildsten 2009). Figure 2 shows the time evolution of mass fractions, X, for each of the eleven isotopes in the `subch` network for three different `burn_cell` simulations. This zone, too, is initialized at $T = 3 \times 10^8 K$ and $\rho = 1 \times 10^6 \frac{g}{cm^3}$. One simulation is run without ^{14}C and ^{14}N, one with some ^{14}N, and the last with both ^{14}C and ^{14}N. If Shen & Bildsten's theory is correct, we shouldn't see the dashed and dotted lines overlay the solid lines, but dashed and dotted lines following different paths and implying that there is a notable change in each of the simulations. In Figure 2, seeing a combination of solid, dashed, and dotted lines at different orders of magnitudes for many elements implies that the incorporation of ^{14}C and ^{14}O is important.

In addition to the mass fraction evolution, the rate of energy generated by the zone in the `burn_cell` simulation is plotted as a function of time in Figure 3. Once more, this is done for a simulation without ^{14}C and ^{14}N, adding only ^{14}N, and adding both ^{14}C and ^{14}N. From Figure 3 one can see that in the
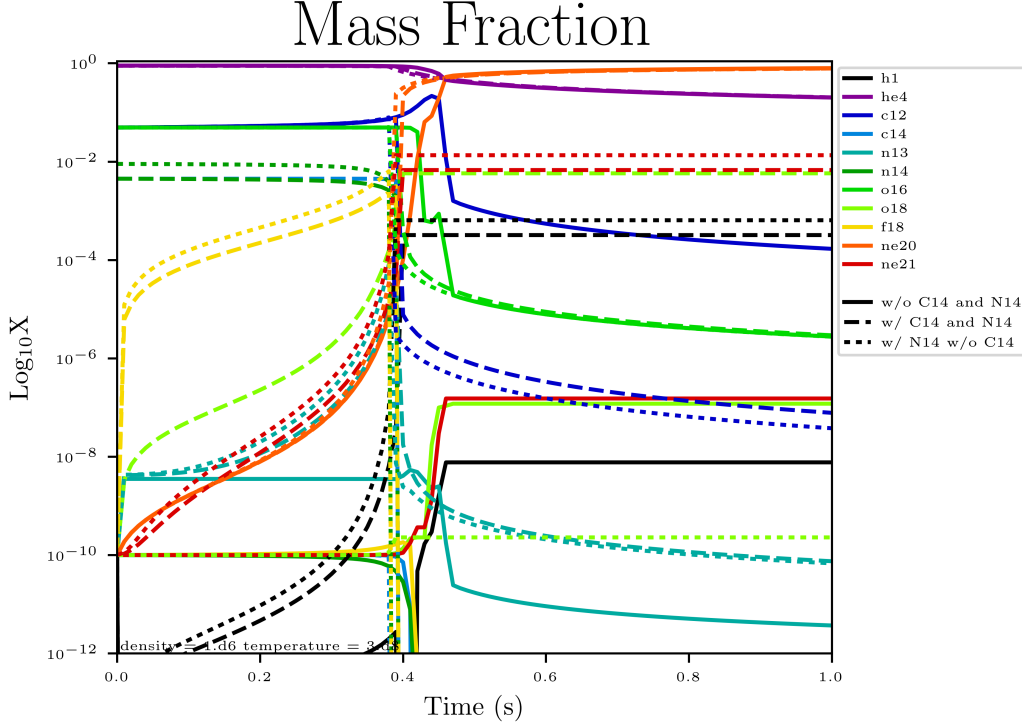
Figure 2. Mass fraction, X, evolution over time for the 11 elements (differentiated by color) in the `subch` network for three different `burn_cell` simulations: one without ^{14}C and ^{14}O (solid lines), one with both ^{14}C and ^{14}O (dashed line), and with ^{14}O but no ^{14}C (dotted line). Notice the large change in ^{12} and ^{21} between the simulations.

simulations with ^{14}C and ^{14}N, the energy generated by this zone peaks sooner and has a lower peak. This shows that when ^{14}C and ^{14}O are incorporated into the simulations of Type Ia SNe, they will generate energy faster, use their nuclear energy more quickly, and have a smaller maximum energy generation rate than simulations without these elements. This is another nudge in the direction of running a full scale simulation.

4.3. *Multi-dimensional simulations with Castro*

The Castro code will be used to first test the `subch` network in one dimension to see if an increase in temperature will ignite a detonation and push it across a layer of helium. A detonation occurs in a star when a thermonuclear runaway causes a supersonic shockwave to move through a medium. If a denotation occurs, then the Castro code will be used to simulate the star in two dimensions. This can then be compared to simulations of stars using other networks and the results can be compared.

4.3.1. *1-Dimensional Simulations*

Using the Castro science problem called "Detonation", a simulation of a shock wave propagating from left to right was initialized with the `subch` network. The layer of helium that this wave is propagating through has a density of $\rho = 1^6 \frac{g}{cm^3}$, has a shock wave with a temperature of $T = 2 \times 10^9 K$ (on the left), and has a resting temperature of $T = 0.05 \times 10^9 K$ (on the right). As shown in Figure 4, the energy released from nuclear reactions in the detonation powers a wave to the right side of the screen and off of the page.
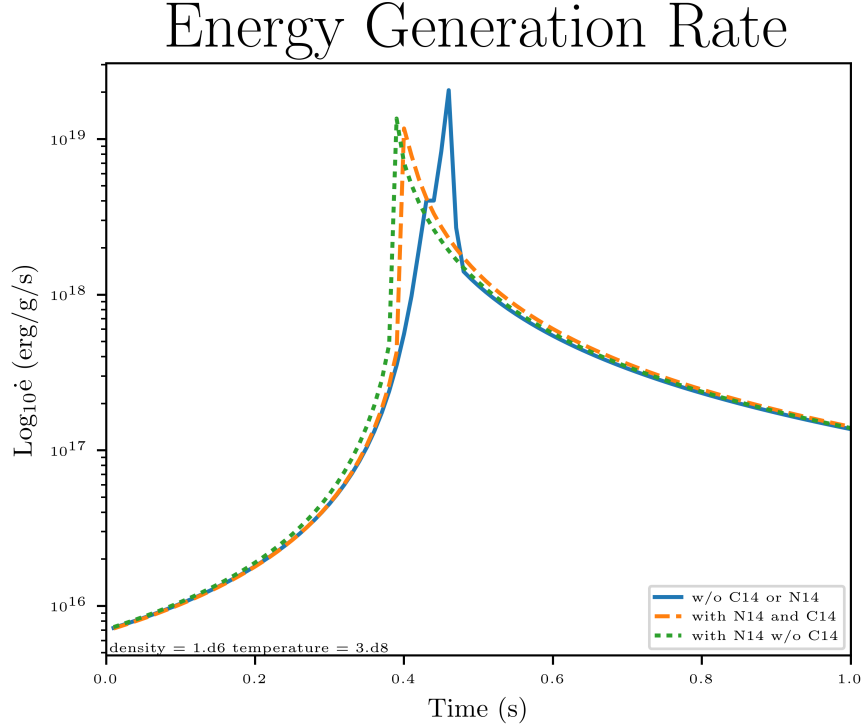
Energy Generation Rate

Figure 3. The rate of energy generated by the zone in the `burn_cell` simulation as a function of time for the run without ^{14}C and ^{14}O (solid lines), with both ^{14}C and ^{14}O (dashed line), and with ^{14}O but no ^{14}C (dotted line).

Now, knowing that a mild temperature perturbation can ignite a helium layer, this simulation can be taken to two dimensions, which is a big step. These one dimensional simulations take a couple minutes to run on an average computer but the two dimensional simulations will take much longer, even on a much larger computer.

4.3.2. *2-Dimensional Simulations*

The two dimensional simulations are completed by wrapping a ^{12}C and ^{16}O WD core in a thick layer of ^{4}He and simulating it in axisymmetric coordinates. The burning is initiated by a hot temperature perturbation at the interface between the helium shell and the core along the north pole of the star. Figure 5 shows this setup.

The domain of simulation is $1.25 \times 10^9 cm$ wide by $2.5 \times 10^9 cm$ high, 3 levels of refinement are used (more levels, more accurate, longer run time), a perturbation temperature factor of 80, a perturbation radius factor of 8, centered at a distace of 0.35 billion centimeters from the center from the star. Using the `subch` network to simulate this, the images in Figure 5 resulted. At the top of the star in the second image, it is clear that the shock wave is propagating across the helium layer of the WD and that the front of the shock wave has a temperatures near 2.5×10^9 Which is very high and very promising.
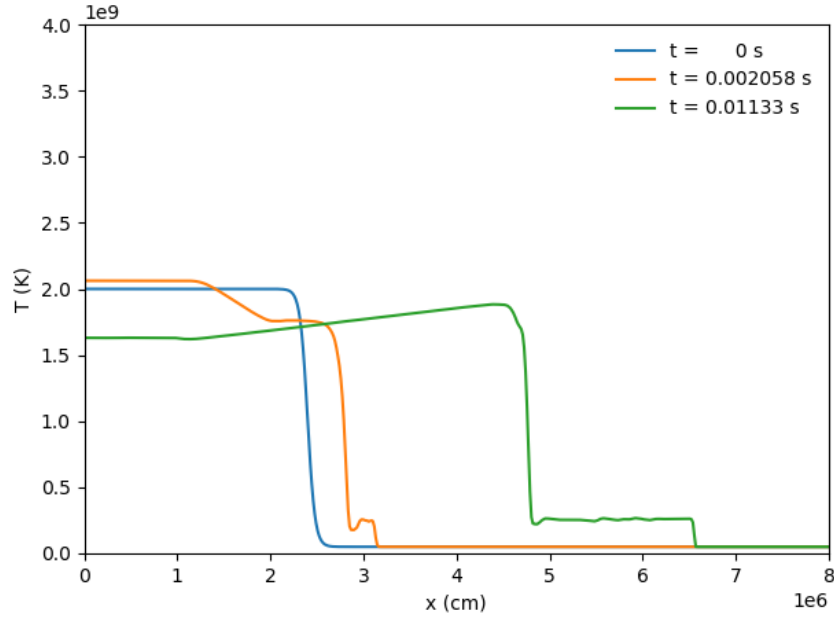
8

Figure 4. The above images depict a detonation wave (shown by a shelf of temperature on the left at 2 billion K) propagating in the right direction at the beginning of the simulation (Figure (a)), after 0.002 seconds (Figure (b)), and after 0.01 seconds (Figure (c)).

5. CONCLUSION

Shen & Bildsten's paper brought light that simulations of Type Ia SNe needed more work, motivating the investigation narrated in this report. After checking the accuracy of codes used, simulations using a network of nuclear reaction rates based off of the Shen & Bildsten paper were used in a one zone simulation, moving to a one dimensional simulation, and culminating in an insightful two dimensional simulation (Shen & Bildsten 2009). After a few months of struggling with and manipulating the Castro code and inputs value, we reminded ourselves of the importance of setting accurate lower limits for qualities such as density and reminding the code to reevaluate the adaptive mesh refinement gridding frequently. Now that the simulation is running, it is shown that the shock wave will propagate through the helium layer of the WD. Simulations are still running so we will have to wait for them to finish before we can see if the core detonates and causes the SNe.

The next steps moving forward will be to perform this in two dimensions with rotation involved comparing the results between runs with different Helium layer masses. Afterwards, this may be promoted to a three dimensional simulation. Using these results we can motivate fellow scientists to use their codes to retrieve the information about brightness curves and spectra so that observational astronomer can use them for calculating astronomical distance. Through the generation of better simulations, the scientific community gains better results and can produce excellent science.
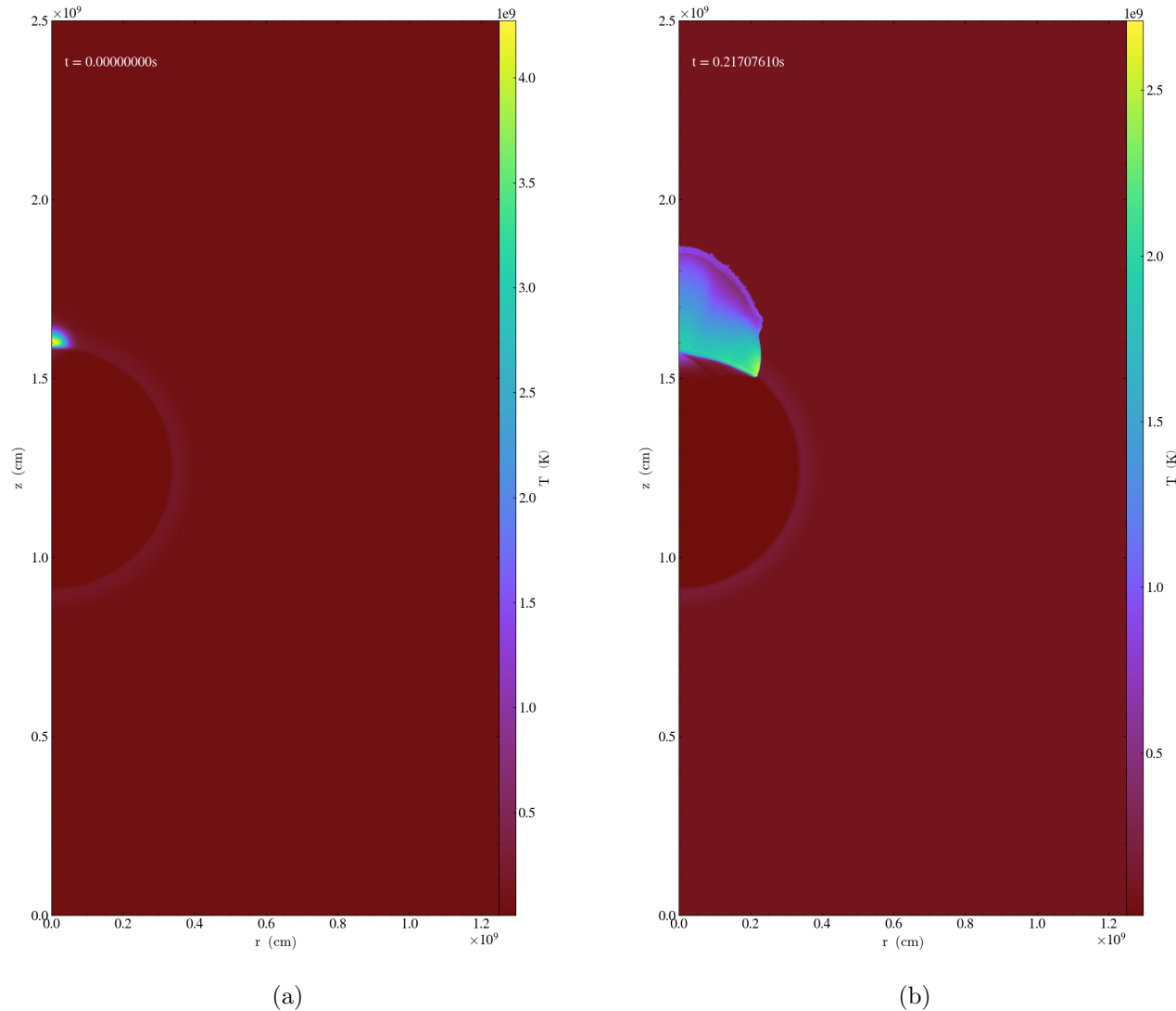
Figure 5. These plots were created using `amrvis` which can be found in the AMReX coding package (the AMReX Development Team et al. 2019). They depict the WD as a half circle in the left middle and use color to display the temperature in the plane. A redder color is a cooler temperature and a yellow color represents warmer temperatures. Note that the values associated with the color scale of the temperature may change between pictures.

6. ACKNOWLEDGEMENTS

I would like to thank Dr. Donald Willcox and Dr. Adam Jacobs for all of their help and guidance in regards to the usage of Pynucastro, Microphysics, and Castro. I would like to thank Dr. Anja von der Linden and Elizabeth Bojza for reading my thesis. Lastly, I would like to offer my greatest thanks to Dr. Michael Zingale for helping me with this thesis, for being my researchadvisor for the past two years, and for being an absolutely amazing mentor.

REFERENCES

Almgren, A. S., Beckner, V. E., Bell, J. B., et al. 2010, ApJ, 715, 1221, doi: 10.1088/0004-637X/715/2/1221

Burrows, A., Dolence, J. C., & Murphy, J. W. 2012, The Astrophysical Journal, 759, 5, doi: 10.1088/0004-637x/759/1/5

Cyburt, R. H., Amthor, A. M., Ferguson, R., et al. 2010, The Astrophysical Journal Supplement Series, 189, 240, doi: 10.1088/0067-0049/189/1/240

Dolence, J. C., Burrows, A., Murphy, J. W., & Nordhaus, J. 2013, The Astrophysical Journal, 765, 110, doi: 10.1088/0004-637x/765/2/110

Fink, M., Hillebrandt, W., & Röpke, F. K. 2007, A&A, 476, 1133, doi: 10.1051/0004-6361:20078438

Jacobs, A. M., Zingale, M., Nonaka, A., Almgren, A. S., & Bell, J. B. 2016, ApJ, 827, 84, doi: 10.3847/0004-637X/827/1/84

Katz, M. P., Zingale, M., Calder, A. C., et al. 2016, The Astrophysical Journal, 819, 94, doi: 10.3847/0004-637x/819/2/94

Kromer, M., Sim, S. A., Fink, M., et al. 2010, ApJ, 719, 1067, doi: 10.1088/0004-637X/719/2/1067

Perlmutter, S., Aldering, G., Goldhaber, G., et al. 1999, The Astrophysical Journal, 517, 565, doi: 10.1086/307221

Phillips, M. M. 1993, ApJL, 413, L105, doi: 10.1086/186970

Riess, A. G., Filippenko, A. V., Challis, P., et al. 1998, The Astronomical Journal, 116, 1009, doi: 10.1086/300499

Shen, K. J., & Bildsten, L. 2009, ApJ, 699, 1365, doi: 10.1088/0004-637X/699/2/1365

Strang, G. 1968, SIAM Journal on Numerical Analysis, 5, 506, doi: 10.1137/0705041

the AMReX Development Team, Almgren, A., Beckner, V., et al. 2019, AMReX-Codes/amrex: AMReX 19.05.1, doi: 10.5281/zenodo.2754709. https://doi.org/10.5281/zenodo.2754709

the StarKiller Microphysics Development Team, Bishop, A., Fields, C. E., et al. 2019, starkiller-astro/Microphysics: Microphysics 19.05, doi: 10.5281/zenodo.2656476. https://doi.org/10.5281/zenodo.2656476

Timmes, F. X. 2019, Nuclear Reaction Networks. http://cococubed.asu.edu/code_pages/burn.shtml

Willcox, D. E., & Zingale, M. 2018, arXiv e-prints, arXiv:1803.08920. https://arxiv.org/abs/1803.08920

Zingale, M., Nonaka, A., Almgren, A. S., et al. 2013, ApJ, 764, 97, doi: 10.1088/0004-637X/764/1/97